

# Mitigating long transient time in deterministic systems by resetting

Arnob Ray,<sup>1,\*</sup> Arnab Pal,<sup>2,†</sup> Dibakar Ghosh,<sup>1</sup> Syamal K. Dana,<sup>3,4</sup> and Chittaranjan Hens<sup>1,‡</sup>

<sup>1</sup>*Physics and Applied Mathematics Unit, Indian Statistical Institute, 203 B. T. Road, Kolkata 700108, India*

<sup>2</sup>*School of Chemistry, Faculty of Exact Sciences & The Center for Physics and*

*Chemistry of Living Systems, Tel Aviv University, Tel Aviv 6997801, Israel*

<sup>3</sup>*Centre for Mathematical Biology and Ecology, Department of Mathematics, Jadavpur University, Kolkata 700032, India*

<sup>4</sup>*Division of Dynamics, Faculty of Mechanical Engineering,*

*Lodz University of Technology, 90-924 Lodz, Poland*

(Dated: July 20, 2020)

How long does a trajectory take to reach a stable equilibrium point in the basin of attraction of a dynamical system? This is a question of quite general interest, and has stimulated a lot of activities in dynamical and stochastic systems where the metric of this estimation is often known as the transient or first passage time. In nonlinear systems, one often experiences long transients due to their underlying dynamics. We apply resetting or restart, an emerging concept in statistical physics and stochastic process, to mitigate the detrimental effects of prolonged transients in deterministic dynamical systems. We show that stopping an ongoing process at intermittent time only to restart all over from a spatial control line, can dramatically expedite its completion, resulting in a huge decrease in mean transient time. Moreover, our study unfolds a net reduction in fluctuations around the mean. Our claim is established with detailed numerical studies on the Stuart-Landau limit cycle oscillator and chaotic Lorenz system under different resetting strategies. Our analysis opens up a door to control the mean and fluctuations in transient time by unifying the original dynamics with an external stochastic or periodic timer, and poses open questions on the optimal way to harness transients in dynamical systems.

Transient time is unequivocally an important attribute of dynamical systems. In simple words, transient time (TT) quantifies the time it takes for a trajectory to reach from any point P to another point Q, specifically from an initial state to an attractor i.e. stable oscillation or an equilibrium point. In recent times, statistics of TT has been extensively studied in complex dynamical systems [1–6], climate models [7, 8], ecology [9–12], signal propagation in networks [13, 14] and extreme events like catastrophes or species extinction [15–17]. TT has also been a key ingredient to understand critical transitions from one stable ecosystem state to another often known as tipping [18] or regime shift [19]. In ecology, faster convergence to stable solutions under external perturbations is known to be of severe importance to sustain resilience [20, 21]. Similarly, one can ask whether it is possible to operate a power grid network [22] with a faster realization of synchrony to avoid a failure. Thus, the intriguing questions are how to tailor *generic strategies* to understand optimization and control of transient time in natural and engineered systems.

Transient time is also a subject of immense interest in statistical physics and stochastic process. Therein, it is often known as the first passage time (FPT) which measures the completion time of a process (see [23–26] for extensive reviews). Despite many years of rigorous studies, efforts are still being made in search of finding new protocols to make the FPT processes more efficient [27–31]. Recently, it has been observed that completion of a

FPT process can be expedited by resetting it intermittently and starting afresh [32–49]. This problem is known as first passage under restart or resetting and has led to a myriad of interesting phenomena with an overarching stream of applications in non-equilibrium systems [32], biological and chemical processes [40, 46], randomized search algorithms in computer science [41, 42], search and foraging theory [44, 45, 48, 49]. The pinnacle of these studies is perhaps the expedition of the mean FPT by choosing a careful restart mechanism.

Despite a wide array of studies made in noisy systems, a little knowledge exists, in literature, on the impact of resetting strategies in deterministic dynamical systems. For instance, resetting can be understood as restoration of an apex predator or other species population in the hierarchical levels of a food chain for biodiversity conservation [50] or a catastrophe [51]. Naturally, the question arises whether resetting can now be used as a *control strategy* for TT in deterministic dynamics where the target is a stable steady state, a limit cycle or a chaotic orbit. Furthermore, it is not apparent how to implement the resetting mechanism since the intrinsic dynamics is deterministic and thus, restarting the system from the same initial condition can not improve the transient time. To address these challenges, in this article, we numerically study TT in the presence of resetting. We seek for efficient protocols based on resetting to mitigate the effects of long transient time in dynamical systems having stable equilibrium points and furthermore strive to make them optimal. In particular, our results are illustrated with two canonical models of deterministic systems namely a Stuart-Landau oscillator (denoted by  $\mathbb{M}_1$ ) and the Lorenz system (denoted by  $\mathbb{M}_2$ ). The central

\* Equal contribution

† Equal contribution; [arnabpal@mail.tau.ac.il](mailto:arnabpal@mail.tau.ac.il)

‡ [chittaranjanhens@gmail.com](mailto:chittaranjanhens@gmail.com)

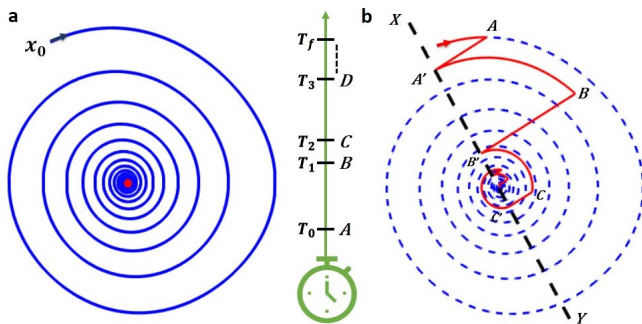


FIG. 1. Illustrative description of resetting strategy. (a) Trajectory of a deterministic system that starts from the initial state  $\mathbf{x}_0$  and reaches an equilibrium point (red dot). (b) Trajectory under resetting is projected momentarily ( $A \rightarrow A'$ ,  $B \rightarrow B'$  and so on) on the control line  $XY$  (black dashed line) chosen from the basin  $\mathcal{B}_A$  and passing through the equilibrium point. Resetting events occur at random times  $T_0, T_1, T_2, \dots, T_f$  (as shown by the clock), where the time intervals  $T_i - T_{i-1}$  are taken from a distribution  $f_R(t)$ . The trajectory with resets (red line) is superimposed on the unhindered trajectory (dashed blue line).

finding of our study reveals that resetting on a spatial *control line* which is constructed arbitrarily through the stable equilibrium point(s) in the basin of attraction dramatically *reduces the mean and fluctuations* in transient time and thus outperforms the completion.

*Transient time.*— Consider an autonomous system spanned in a basin  $\mathcal{B}_A$  and described by

$$\dot{\mathbf{x}} = F(\mathbf{x}, \boldsymbol{\mu}), \quad (1)$$

where  $\mathbf{x}$  is the state variable,  $F$  is a smooth vector field with dimension  $n$  and  $\boldsymbol{\mu}$  is the system parameter. If the system has a monostable point attractor i.e., a stable equilibrium point  $\mathcal{A}$  (say, the target point), then  $TT(\mathbf{x}_0)$  is the time required, in the absence of resetting, to reach the stable attractor of the system from randomly chosen initial points  $\mathbf{x}_0 \in \mathcal{B}_A$ . Following [52–55], the metric for  $TT$  is defined as

$$TT(\mathbf{x}_0) = \inf\{t : \|\phi^{TT}(\mathbf{x}_0) - \mathcal{A}\| < \epsilon, \}, \quad (2)$$

where  $\|\cdot\|$  denotes the Euclidean distance and we assume that the system evolves through a time evolution operator  $\phi$  and reaches to  $\phi^{TT}(\mathbf{x}_0)$  at a time  $t > 0$ . Further, we set  $\epsilon$  with a pre-defined threshold which is chosen arbitrarily small so as to characterize an approximate proximity of the numerical trajectory to the asymptotically stable equilibrium point  $\mathcal{A}$ . The set of transient time over the initial conditions in  $\mathcal{B}_A$  is then simply given by  $\{TT(\mathbf{x}_0), \forall \mathbf{x}_0 \in \mathcal{B}_A\}$  (Sec. I in [56]).

*Resetting protocol & control line.*— Canonical restart mechanisms, in statistical physics, usually set the configuration of a system to its initial state after a random time which is drawn from a distribution given by  $f_R(t)$  [32, 57–62]. Herein, resetting the process to the initial condition is an impediment due to the strong determinism encoded

in the underlying dynamics. To circumvent this issue, we reset or project the dynamics along a line, which we define as a *control line* in  $\mathcal{B}_A$  but passing through the equilibrium point  $\mathcal{A}$ . To illustrate the concept, we refer to Fig. 1a, where we have considered a trajectory of the uninterrupted process that starts from the initial condition  $\mathbf{x}_0$ .  $TT(\mathbf{x}_0)$  denotes the time required by the trajectory starting from  $\mathbf{x}_0$  to reach the fixed point (red dot) within a precision of  $\epsilon$ . The control line  $XY$  (black dashed line, Fig. 1b) is constructed at a random angle  $\theta \in (0, 2\pi)$  but passing through  $\mathcal{A}$  (red dot). We stop the dynamics e.g., at time  $T_0$  drawn from  $f_R(t)$  and reset the current position (say,  $A$ ) to a point (say,  $A'$ ) on the control line by projecting it normally. Subsequently, the dynamics starts from the point  $A'$ . The next time interval  $T_1 - T_0$  is again drawn from the density  $f_R(t)$  and the procedure is repeated. The resulting trajectory after several resets (i.e., with projections on the control line) at coordinates  $A, B, C$  and  $D$  is shown by the solid line (red line). The process ends when the condition  $\|\phi^{TT}(\mathbf{x}_0) - \mathcal{A}\| < \epsilon$  is satisfied for the *first time* and we denote this net transient time as  $TT_R$ . Against this backdrop, we study statistics of  $TT_R$  with different choices of  $f_R(t)$  for systems,  $\mathbb{M}_1$  and  $\mathbb{M}_2$ , which we introduce now in brief.

*Stuart-Landau (SL) oscillator* ( $\mathbb{M}_1$ ).— SL oscillators are abundantly used to understand many fundamental phenomena such as transition to synchrony and pattern formation [63, 64]. The governing equation for such an oscillator reads  $\dot{Z} = (a + i\Omega - |Z|^2)Z$ , where  $Z = x + iy$  is the complex variable and  $\Omega$  is the natural frequency of oscillation. Here,  $a$  is an internal control parameter that determines the state of the system (oscillatory or a steady state). Initial conditions are chosen uniformly from  $\mathcal{B}_A$  in Fig. 2a. Following a linear stability analysis (Sec. II in [56]), it is shown that the system exhibits a stable spiral approaching an equilibrium point  $\mathcal{A} : (0, 0)$  for  $a < 0$  and stable limit cycle for  $a \geq 0$ . We set  $a = -0.01$  and  $\Omega = 1$  so that the system, after a transient time, attains to  $(0, 0)$  shown by the red dot in Fig. 2a.

*Lorenz system* ( $\mathbb{M}_2$ ).— Lorenz system is a benchmark model of chaotic systems [65–67]. Here, the phase space equations are  $\dot{x} = \sigma(y - x), \dot{y} = \rho x - y - xz, \dot{z} = -\beta z + xy$ , where  $\sigma$  and  $\rho$  are the Prandtl and Rayleigh numbers, respectively, while  $\beta > 0$  is the aspect ratio. The system has two symmetric stable equilibrium points  $(\pm\sqrt{\beta(\rho - 1)}, \pm\sqrt{\beta(\rho - 1)}, \rho - 1)$  only if  $1 < \rho < \frac{\sigma(\sigma + \beta + 3)}{\sigma - \beta - 1}$ . For fixed parameters  $\sigma = 10$  and  $\beta = \frac{8}{3}$ , the system exhibits transient chaos in the range of  $\rho \in (13.926, 24.06)$  [56]. Considering  $\rho = 23$ , we obtain two stable fixed points  $\mathcal{A} : \{P_{1,2} = (\pm a, \pm a, b)\}$ , where  $a = 7.65942$ ,  $b = 22.0$ . We observe a riddled basin, with two disjoint basins of attraction for two emerging scrolls in the dynamics, surrounding two separate equilibrium points (red dots) (Fig. 2f).

*Statistics of transient time without resetting.*— To elucidate the effects of resetting, it is important to first study

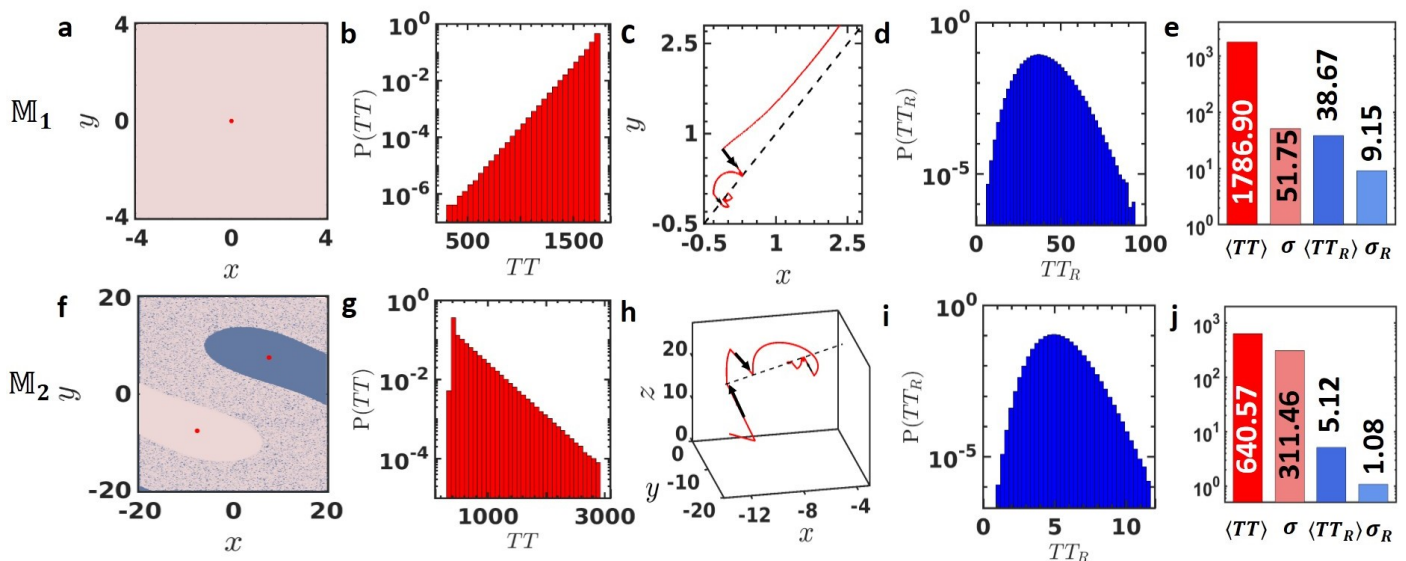


FIG. 2. Basin of attraction:  $\mathcal{B}_A$  with  $\mathcal{A}$  (red dot) for the system (a)  $\mathbb{M}_1$  and (f)  $\mathbb{M}_2$ . Transient time density without resetting:  $P(TT)$  for (b)  $\mathbb{M}_1$  and (g)  $\mathbb{M}_2$ . Phase space trajectories under resetting: Trajectories of the system (c)  $\mathbb{M}_1$ , starting from the co-ordinates (2.5, 3.0) and (h)  $\mathbb{M}_2$ , starting from the co-ordinates  $(-11.74, -4.412, 4.086)$  are depicted by red lines. The black arrows indicate the resets or normal projections to the control line (dashed black line passing through  $\mathcal{A}$ ). Resetting occurs at  $\langle R \rangle = 1$  and  $\langle R \rangle = 0.1$ , respectively, for  $\mathbb{M}_1$  and  $\mathbb{M}_2$ . Transient time density with resetting:  $P(TT_R)$  in the presence of exponential resetting for the systems, (d)  $\mathbb{M}_1$  and (i)  $\mathbb{M}_2$ , respectively, with aforementioned resetting rates. Comparison of mean and fluctuations in transient time without and with resetting: Reduction in  $\langle TT_R \rangle$  and  $\sigma_R$  is observed in the bar plots (with a comparison between their corresponding values) for (e)  $\mathbb{M}_1$  and (j)  $\mathbb{M}_2$  respectively.

the transient time statistics of the underlying systems. To this end, we simulate  $\mathbb{M}_1$  and  $\mathbb{M}_2$  using the 4<sup>th</sup> order Runge-Kutta method while starting from their individual basin of attraction ([56]).  $\mathbb{M}_1$  is a monostable system and has stable spiral trajectory while  $\mathbb{M}_2$  is a 3-dimensional bistable system in which two stable fixed points appear together with two separated and intermingled basins. The system either converges to a single fixed point (for  $\mathbb{M}_1$ ) or fixed points (for  $\mathbb{M}_2$ ) followed by a damped oscillation or a transient chaotic phase for the chosen parameters. Integrating the systems from  $5 \times 10^6$  initial conditions, we have tracked the entire set of reaching time to the vicinity of stable equilibrium points following the condition (given by Eq. 2) with  $\epsilon = 10^{-9}$  set for both the models. To capture the appropriate statistics of  $TT$ , we have scanned the entire basin with a finite resolution, however, discarding the initial conditions which set off from a distance smaller than  $10^{-5}$  from the targeted fixed point. The resulting density functions are shown in Fig. 2b ( $\mathbb{M}_1$ ) and Fig. 2g ( $\mathbb{M}_2$ ). We observe from Fig. 2b that  $P(TT)$  is supported from above. This is because, in  $\mathbb{M}_1$ ,  $TT$  increases exponentially as a function of the Euclidean distance between the initial and targeted state before it saturates to a threshold point which in turn corresponds to the upper bound ([56]). Note that such a relationship is not pertinent to model  $\mathbb{M}_2$ . However, there the transient time is exponentially distributed (Fig. 2g) which is a characteristic feature of chaotic systems [1, 3].

*Transient time under resetting.*— To employ resetting on the underlying dynamics, we first choose the resetting time density to be exponential so that  $f_R(t) = \langle R \rangle^{-1} e^{-t/\langle R \rangle}$  which essentially means that resetting occurs at a rate  $1/\langle R \rangle$  [32]. As outlined before, we first construct the control line in each case and set them fixed for the entire simulation. For  $\mathbb{M}_1$ , the control line is chosen diagonally along the basin and passes through  $\mathcal{A} : (0, 0)$  (black dashed line in Fig. 2c). Figure 2c shows a representative trajectory (red line) with multiple attempts of resetting (black arrows) at a rate  $\langle R \rangle^{-1} = 1.0$ . The resulting distribution of  $TT_R$  (Fig. 2d) immediately reveals two key observations: reduction in both the mean transient time  $\langle TT_R \rangle$  and fluctuations  $\sigma_R \equiv \sqrt{\langle TT_R^2 \rangle - \langle TT_R \rangle^2}$  around the mean. Here, for the current choice of parameters, we noted a dramatic speed up of  $\sim 46$  and  $\sim 6$  times for the mean and fluctuations, respectively (Fig. 2e).

A similar picture is delineated for model  $\mathbb{M}_2$  in Fig. 2h-j. In this case, there is some freedom in the choice of the control line since we have two equilibrium points (which are also the targets)  $P_1$ , and  $P_2$ . The control line can be drawn through either of the equilibrium points or connecting both. We choose the latter case and the resetting procedure is conducted identically at a rate  $\langle R \rangle^{-1} = 10$  (for the details of the former choice, Sec. V in [56]). Collecting the data statistics of  $TT_R$ , we plot a histogram in Fig. 2i, which estimates that resetting over-performs the mean by  $\sim 125$  folds. Alike  $\mathbb{M}_1$ , we find a significant reduction ( $\sim 288$  times) in the fluctuations for  $\mathbb{M}_2$

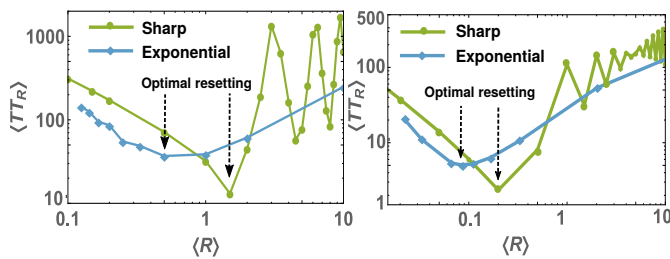


FIG. 3. Plot of  $\langle TT_R \rangle$  as a function of  $\langle R \rangle$  for  $\mathbb{M}_1$  (left panel) and  $\mathbb{M}_2$  (right panel). Resetting times are chosen from exponential (diamond markers) and sharp distribution (circle markers). Sharp resetting reduces  $\langle TT_R \rangle$  more efficiently than the exponential at the optimal time  $\langle R^* \rangle$ .

(Fig. 2j).

To show that indeed this behavior is generic, we now adapt a different strategy where resetting takes place always after a fixed time  $\langle R \rangle$  so that  $f_R(t) = \delta(t - \langle R \rangle)$ . This is often known as the sharp resetting which was proven to be the most time-efficient protocol in stochastic systems [36, 39, 45]. Again, the highlighting features here are the decrements in mean and fluctuations in transient time (see Fig. 3). Manifesting the control line protocol, we find that sharp restart reduces the mean and fluctuation by  $\sim 55$  and  $\sim 152$  folds for  $\mathbb{M}_1$  when  $\langle R \rangle = 1$ . Similarly, for  $\mathbb{M}_2$ , we observe a speed up of  $\sim 106$  for the mean and  $\sim 438$  folds for the fluctuations when performing at a rate  $\langle R \rangle = 0.1$  ([56]).

To delve deeper, we now scan  $\langle TT_R \rangle$  as a function of  $\langle R \rangle$  in Fig. 3 for both the resetting schemes. When  $\langle R \rangle$  is small, the system resets too frequently so that the trajectory is effectively confined near the control line and the transient time is achieved by these short excursions. On the other hand, when  $\langle R \rangle$  is large, the waiting time between resetting events increases. In other words, there is hardly any resetting event and the completion is achieved typically by the original dynamics. For sharp resetting (circle marked green lines), markedly distinct oscillatory behavior emerges when  $\langle R \rangle$  often becomes the integer multiple or half integer multiple of the intrinsic time period of  $\mathbb{M}_1$  (Sec. IV in [56]). This happens since sharp resetting is a periodic process and is always conducted after a fixed time  $\langle R \rangle$ . On the other hand, for  $\mathbb{M}_2$ , we do not observe any systematic pattern due to its aperiodic nature. For exponential resetting, variation of  $\langle TT_R \rangle$  as a function of  $\langle R \rangle$  are shown by the diamond marked blue lines in the same figure where the qualitative features are found to be similar. However, oscillations are not present here since  $f_R(t)$  is a continuous distribution and thus the waiting time between resetting events are not multiples of the underlying time period.

In the intermediate regime of  $\langle R \rangle$ , in both the cases, the trajectory explores its intrinsic dynamics between consecutive resetting events. The combined effect essentially leads to a drastic decrease in  $\langle TT_R \rangle$  (see Fig. 3). Quite interestingly, we see emergence of an optimal re-

setting rate  $\langle R^* \rangle$  such that  $\frac{d\langle TT_R \rangle}{d\langle R \rangle}|_{\langle R^* \rangle} = 0$ . In our set up, we find that for  $\mathbb{M}_1$  ( $\mathbb{M}_2$ ), the optimal transient times  $\langle TT_R^* \rangle$  for the exponential and sharp resetting are  $\approx 36.86$  (5.06) and  $\approx 13.5$  (2.35) respectively. The above analysis clearly indicates that sharp resetting could work more efficiently to reduce transient time than the exponential resetting at the optimal condition.

*Discussions and future outlook.*— In this paper, we showcase a first study on the application of resetting in deterministic dynamical systems having prolonged transient time. We show that systematic controlled resetting strategies, which mix and match external stochastic and periodic timers with internal spatial properties, have an ability to facilitate the completion of a process, by reducing mean and fluctuations, which otherwise would hinder. With the aid of numerical simulations, we investigate two paradigmatic non-linear systems under Poisson or exponential and sharp resetting. Noteworthy in this regard is the *dominance of sharp resetting over exponential resetting* at the optimality. While this observation is quite intriguing, future studies to formally establish this result in dynamical systems look like a serious challenge.

To conceptualize resetting in our systems, we have introduced the notion of a *control line* to which the system is projected after each resetting. We have shown that the method of control line performs proficiently for both the models and thus is quite robust. For a homogeneous basin ( $\mathbb{M}_1$ ), the reduction in transient time remains fully invariant on the choice of control line (Sec. V in [56]). However, for  $\mathbb{M}_2$ , the transient time depends clearly on the choice of the control line which here can be of three kinds passing through  $P_1$  or  $P_2$  (or both). For the first two cases, the system reaches to their respective equilibrium points while for the third case the probability to converge to any of these equilibrium points is equally shared. It is important to point out that the models chosen here show behavioral shift (steady state to oscillation, periodic or chaotic) when we change the system parameters to a critical value. Remarkably, even near the onset of critical transitions, we find that resetting remains beneficial for a range of parameters (Sec. VI in [56]).

Concluding, we stress that we have shown extensively that persistent resetting can reverse the deleterious effects of long transient time in autonomous systems. Notably, in this first case study, we have assumed resetting process to be instantaneous in order to keep congruence with the original idea of resetting. However, to adapt realistic scenarios, future studies need to be carried out to explore the effects of a time overhead or delay due to resetting [68]. Nonetheless, we believe that the qualitative key features observed here should remain invariant. Thus, indeed, resetting can operate as a powerful assay to regulate transient time in complex systems.

*Acknowledgments.*— The authors would like to thank Sarbendu Rakshit for interesting discussions and notable comments. A. P. gratefully acknowledges support from the Raymond and Beverly Sackler Post-Doctoral Schol-

arship at Tel-Aviv University. C.H. is supported by DST- INSPIRE Faculty Grant No. IFA17-PH193.

# Supplemental Material: “Mitigating long transient time in deterministic systems by resetting

## CONTENTS

I.	Notation and definition of Transient Time	7
II.	Linear stability analysis: $\mathbb{M}_1$ and $\mathbb{M}_2$	7
	A. Eigenvalue analysis of $\mathbb{M}_1$	7
	B. Eigenvalue analysis of $\mathbb{M}_2$	8
III.	Distance and transient time density without resetting	8
	A. Transient time for $\mathbb{M}_1$	8
	B. Transient time for $\mathbb{M}_2$	9
IV.	Emergence of oscillatory behavior under sharp resetting in $\mathbb{M}_1$	9
V.	Behavior of the mean and fluctuations in transient time on the choice of control lines	11
	A. Effect of control lines on $\mathbb{M}_1$	11
	B. Effect of control lines on $\mathbb{M}_2$	12
	1. Effect of fixed control line passing through both $P_1$ and $P_2$	13
	2. Effect of fixed control line passing through $P_1$	13
	3. Effect of fixed control line passing through $P_2$	13
VI.	Impact of control parameters on the transient time near the critical transition	13
	A. System $\mathbb{M}_1$	14
	B. System $\mathbb{M}_2$	15
VII.	Computational method	15
VIII.	Summary of the numerical values used in the main text	16
	References	17

## I. NOTATION AND DEFINITION OF TRANSIENT TIME

A deterministic dynamical system can be captured by an ordinary differential equation of the following form

$$\dot{\mathbf{x}} = F(\mathbf{x}, \boldsymbol{\mu}), \quad (3)$$

where  $F$  represents the vector field,  $\mathbf{x} \in \mathbb{R}^n$  and  $\boldsymbol{\mu}$  is the parameter. Let  $\mathcal{A}$  ( $\subseteq \mathbb{R}^n$ ) be an attractor of the Eq. (3) and corresponding basin of attraction is denoted by  $\mathcal{B}_{\mathcal{A}}$  ( $\subseteq \mathbb{R}^n$ ). Let  $\mathbf{x}_0 = (x_{10}, x_{20}, \dots, x_{n0})^T$  ( $\mathcal{T}$  denotes the transpose of a matrix) be an initial condition at  $t = t_0$  from which the system evolves through a time evolution map  $\phi$  and reaches to  $\phi_{t_0}^t(\mathbf{x}_0)$  at time  $t > 0$ . If  $\mathcal{A}$  is an asymptotically stable equilibrium point, we can write  $\phi_{t_0}^{t \rightarrow \infty}(\mathbf{x}_0) \rightarrow \mathcal{A}$ . For practical purpose, we assume that the system reaches to the close vicinity of the stable attractor  $\mathcal{A}$  in a finite time, say  $TT(\mathbf{x}_0)$  for initial state  $\mathbf{x}_0$ . We call this finite time  $TT(\mathbf{x}_0)$  as *transient time*, which is formally defined as follows

$$TT(\mathbf{x}_0) = \inf\{t : \|\phi^{TT}(\mathbf{x}_0) - \mathcal{A}\| < \epsilon\}, \quad (4)$$

where  $\epsilon$  is a small positive number and  $\|\cdot\|$  denotes the Euclidean distance. One can define this metric  $D$  as  $D(\mathbf{x}, \mathbf{y}) = \sqrt{\sum_{i=1}^n (x_i - y_i)^2}$ , where  $\mathbf{x} = (x_1, x_2, \dots, x_n) \in \mathbb{R}^n$  and  $\mathbf{y} = (y_1, y_2, \dots, y_n) \in \mathbb{R}^n$ . We set  $\epsilon = 10^{-9}$  for our simulations. Now, the set of transient time over the entire basin  $\mathcal{B}_{\mathcal{A}}$  can be constructed as  $\{TT(\mathbf{x}_0), \text{ for all } \mathbf{x}_0 \in \mathcal{B}_{\mathcal{A}}\}$ , i.e.  $\mathbf{x}_0$  is all accessible initial conditions in the basin  $\mathcal{B}_{\mathcal{A}}$ .

## II. LINEAR STABILITY ANALYSIS: $\mathbb{M}_1$ AND $\mathbb{M}_2$

In this section, we present a linear stability analysis for the two paradigmatic models used in the main text namely the Stuart-Landau system ( $\mathbb{M}_1$ ) and the Lorenz system ( $\mathbb{M}_2$ ).

### A. Eigenvalue analysis of $\mathbb{M}_1$

Stuart Landau model ( $\mathbb{M}_1$ ) is described by the following governing equation of motion [66, 67]

$$\dot{Z} = (a + i\Omega - |Z|^2)Z, \quad (5)$$

where  $Z = x + iy$  is the complex variable;  $a$  and  $\Omega$  are the intrinsic parameters of the system. The system has one equilibrium point at  $(0, 0)$ . Now, the Jacobian matrix  $J$  of the system  $\mathbb{M}_1$  at the equilibrium point  $(0, 0)$  is given by

$$J(0, 0) = \begin{bmatrix} a & -\Omega \\ \Omega & a \end{bmatrix}.$$

The characteristic roots of the above Jacobian are  $\lambda_{\pm} = a \pm \Omega i = -0.01 \pm i$ , where  $a = -0.01$  and  $\Omega = 1$ . Therefore, the trivial equilibrium point  $(0, 0)$  is a stable spiral. Here, the system parameter  $a$  determines decay rate. On the other hand, the imaginary part of the eigenvalue  $\Omega$  determines the intrinsic frequency of this decaying oscillation. Thus, the time period of oscillatory behavior during the transient phase, for our current choice of parameters, is given by

$$T(\mathbb{M}_1) \sim \frac{2\pi}{\Omega} \approx 6.28318. \quad (6)$$

We note that the system experiences a critical transition (from stable spiral to a stable limit cycle) at  $a_c \equiv a = 0.0$ .

### B. Eigenvalue analysis of $\mathbb{M}_2$

The governing equation of motion for the Lorenz system ( $\mathbb{M}_2$ ) is given by [66, 67]

$$\begin{aligned} \dot{x} &= \sigma(y - x), \\ \dot{y} &= \rho x - y - xz, \\ \dot{z} &= -\beta z + xy, \end{aligned} \quad (7)$$

where the system parameters are  $\sigma, \rho$ , and  $\beta (> 0)$ . It is easy to see that the system has a trivial equilibrium point  $P_0 : (0, 0, 0)$  which is stable for  $\rho < 1$ . For  $\rho > 1$ , two non-trivial equilibrium points emerge which are given by  $P_1 : (\sqrt{\beta(\rho - 1)}, \sqrt{\beta(\rho - 1)}, \rho - 1)$  and  $P_2 : (-\sqrt{\beta(\rho - 1)}, -\sqrt{\beta(\rho - 1)}, \rho - 1)$ . Now we proceed to calculate the Jacobian matrix  $J$  of the system  $\mathbb{M}_2$  at the equilibrium point  $P_1$ . This gives

$$J(\sqrt{\beta(\rho - 1)}, \sqrt{\beta(\rho - 1)}, \rho - 1) = \begin{bmatrix} -\sigma & \sigma & 0 \\ 1 & -1 & -\sqrt{\beta(\rho - 1)} \\ \sqrt{\beta(\rho - 1)} & \sqrt{\beta(\rho - 1)} & -\beta \end{bmatrix}. \quad (8)$$

One can now immediately write the characteristic equation coming from the Jacobian above, and this reads

$$\lambda^3 + (\beta + \sigma + 1)\lambda^2 + \beta(\rho + \sigma)\lambda + 2\beta\sigma(\rho - 1) = 0. \quad (9)$$

For fixed parameters e.g.,  $\sigma = 10, \beta = \frac{8}{3}$  and  $\rho = 23$ , the characteristic equation Eq. (9) becomes

$$\lambda^3 + \frac{41}{3}\lambda^2 + 88\lambda + \frac{3520}{3} = 0. \quad (10)$$

The roots of the above equation are simply given by  $\lambda = -13.5588; -0.054 \pm 9.3024i$ . Therefore linear stability analysis at the vicinity of  $P_1$  determines that it is a stable spiral. In the same way, one can also show that  $P_2$  is a stable spiral. Note that, the system has a transient chaos phase in a range of  $\rho \in (13.926, 24.06)$  for  $\sigma = 10$  and  $\beta = \frac{8}{3}$  [1]. Increasing  $\rho$  towards the critical transition point ( $\rho_c = 24.06$ ), the duration of chaotic transient phase follows a power law [1–3]. At  $\rho = \rho_c$ , the critical transition occurs and the transient chaos becomes a chaotic attractor.

### III. DISTANCE AND TRANSIENT TIME DENSITY WITHOUT RESETTING

In this section, we discuss in details the quantitative features of the transient time density  $P(TT)$  in the absence of resetting. To obtain the histogram for each model, we have scanned  $5 \times 10^6$  initial conditions from the basin of attraction  $\mathcal{B}_A$ .

#### A. Transient time for $\mathbb{M}_1$

In the case of system  $\mathbb{M}_1$ , we choose our basin span to be  $[-6, 6] \times [-6, 6]$ , and collect the transient time. The resulting density is plotted in Fig. 2b in the main text. From the figure, it becomes evident that the density is supported from above. Moreover, we observe that the probability to get larger values of  $TT$  is higher than the smaller values of  $TT$ . To gain deeper insights, we have investigated the relation between the transient time (of the trajectories taken from initial points in basin to stable equilibrium point) and the Euclidean distance (between initial and target states). The Euclidean distance, metric  $D$ , is described as

$$D(\mathbf{x}, \mathbf{y}) = \sqrt{\sum_{i=1}^n (x_i - y_i)^2}, \quad (11)$$

where  $\mathbf{x} = (x_1, x_2, \dots, x_n) \in \mathbb{R}^n$  and  $\mathbf{y} = (y_1, y_2, \dots, y_n) \in \mathbb{R}^n$ . We collect all  $D$  and  $TT$  for both models and plot them in Fig. 4a. For  $\mathbb{M}_1$ , the transient time increases exponentially as we increase the Euclidean distance ( $TT \sim e^D$ ) till



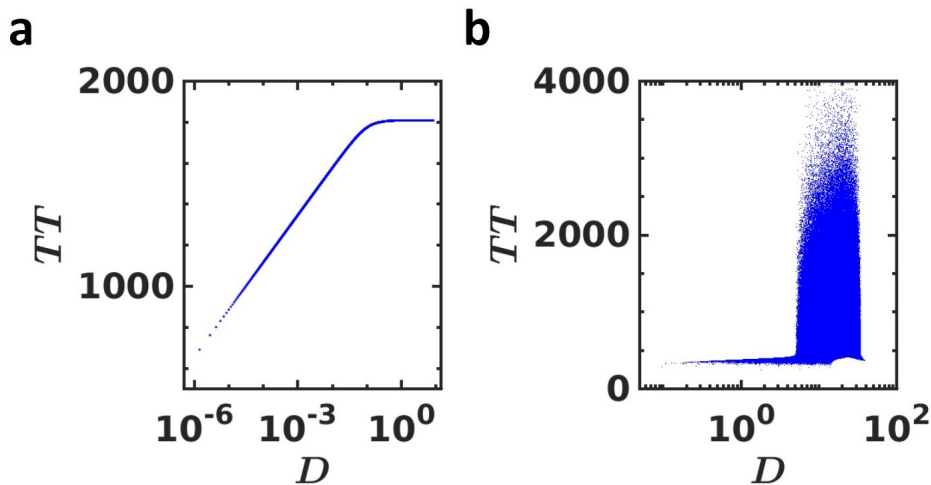


FIG. 4. Variation between  $D$  and  $TT$ : Transient time as a function of  $D$ , the distance between the initial point and the target for  $\mathbb{M}_1$  (panel a) and  $\mathbb{M}_2$  (panel b). For  $\mathbb{M}_1$  (panel a), we find that  $TT$  increases exponentially as a function of  $D$  till it reaches a threshold and then saturates. The threshold value for  $D$  is estimated to be  $\sim 0.6$ . On the other hand, it is clear from panel b ( $\mathbb{M}_2$ ) that there is no such relationship between  $TT$  and the distance  $D$ . Parameter values set for the simulations are for (a)  $a = -0.01, \Omega = 1$ , and for (b)  $\sigma = 10, \rho = 23, \beta = \frac{8}{3}$

some threshold  $D^* < 0.6$ . Beyond this certain distance ( $D > D^*$ ), all the trajectories take significant small time to reach to the surface of the circle having radius ( $D \approx D^*$ ). In effect,  $TT$  saturates around approximately 1800 for the current choices of parameters. So, for  $D < D^*$ ,  $TT$  has an exponential growth and beyond, it saturates to a specific value. This essentially tells that no matter where one starts in the basin, the maximum  $TT$  that could be achieved is approximately similar (with some small fluctuations) to that of starting from  $D^*$ . Thus, the probability density function of the transient time is bounded from above by this maximum value of  $TT$ .

### B. Transient time for $\mathbb{M}_2$

In  $\mathbb{M}_2$ , we take the size of basin of attraction to be  $[-20, 20] \times [-20, 20] \times [0, 30]$ . Performing a similar analysis as above for the averaging, we have plotted the histogram for  $TT$  in Fig. 2g in the main text. Here, we find that  $P(TT)$  is an exponential distribution, which is a fingerprint of chaotic systems [1].

However, we did not find any direct relationship between  $TT$  and  $D$  for the Lorenz system. In higher  $D$ ,  $TT$  ranges from low value 500 to higher value 4000. It is clear that  $D \gtrsim 5$ , the scatter points are dense around 500-2500 (see Fig. 4b). The less number of points appear in higher value of  $TT$  ( $TT \gtrsim 3000$ ). Therefore,  $P(TT)$  is less probable at higher values of  $TT$ . This information is consistent with the form of  $P(TT)$  [see Fig. 2g in the main text].

## IV. EMERGENCE OF OSCILLATORY BEHAVIOR UNDER SHARP RESETTING IN $\mathbb{M}_1$

In this section, we briefly discuss the origin of the oscillatory behavior of  $\langle TT_R \rangle$  under sharp resetting mechanism in  $\mathbb{M}_1$ . This protocol essentially asserts that one resets the system always after a fixed  $\langle R \rangle$  amount of time. Note that this oscillatory behavior is markedly different than the exponential resetting where we observed a simple non-monotonic behavior (Fig. 3 in the main text). To explain this, at first, we accumulated  $\langle TT_R \rangle$  for different values of  $\langle R \rangle$  shown in Fig. 5a (Table). Moreover, we recall from Sec. II A that the intrinsic periodicity of  $\mathbb{M}_1$  model is around  $T = \frac{2\pi}{\Omega} \approx 6.3$  for  $\Omega = 1$  (Eq. 6). We now identify from the table (Fig. 5a) the *light red marked rows* that satisfy

$$\langle R \rangle \approx \frac{nT}{2}, n = 1, 2, 3, \dots, \quad (12)$$

where  $T$  is the intrinsic period. From the red marked rows of the table, we identify the mean resetting time  $\langle R \rangle$ : 3, 6.5, 9.5 for which we respectively find  $\langle TT_R \rangle \approx (1343.21, 1310.01, 1716.4)$ , which are notably much higher than the transient time one would expect under resetting. Essentially, these mean resetting times commensurate with the

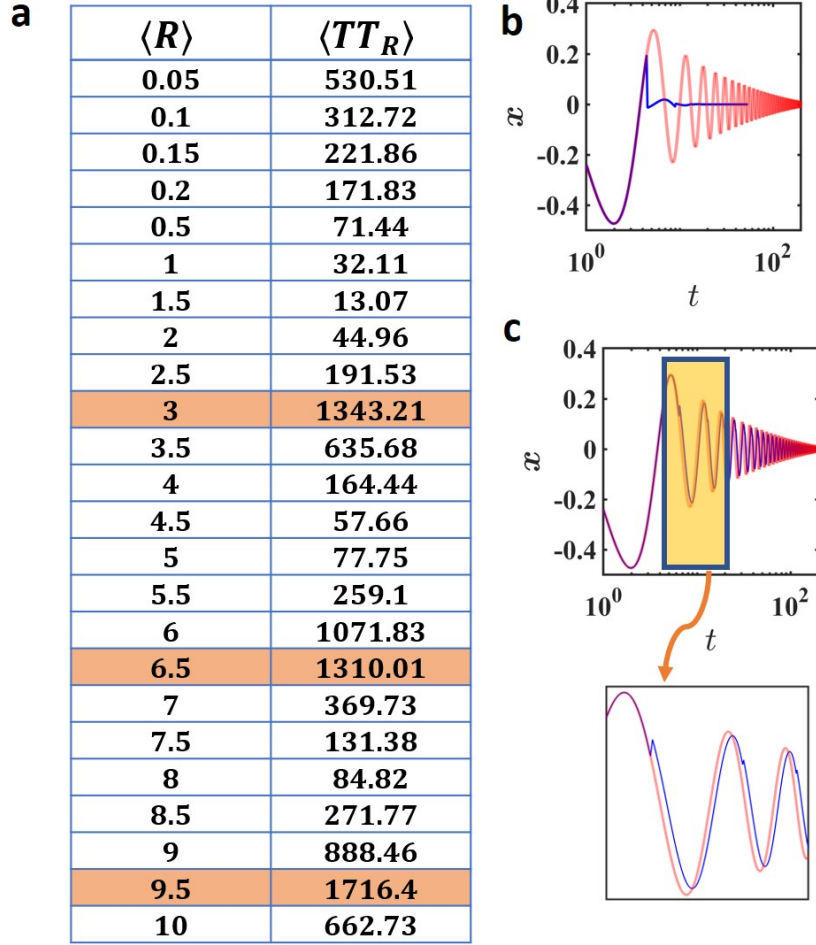


FIG. 5. Panel (a): Table for mean transient time as a function of  $\langle R \rangle$  (in the case of sharp resetting) for model  $M_1$ . Marked in red are the rows for which the period  $\langle R \rangle$  of sharp resetting is approximately close to the half or integer function of the intrinsic time period ( $T$ ) of the original process. Time series (trajectory in  $x$ -coordinate as a function of time) without (in red) and with (in blue) resetting: in panel (b), we have plotted the trajectory for  $\langle R \rangle = 4.5$  against the original trajectory. We see a clear distinction between the original and resetting induced trajectories. In particular, the plot shows that the trajectory with resetting reaches the target much faster than the original one thus resulting in a lower  $\langle TT_R \rangle$ . In panel (c), we have plotted the trajectories when  $\langle R \rangle = 6.5$  (recall  $T \approx 6.3$ ). We see that the trajectories almost follow each other (also see the inset where we have zoomed a part of both the signals) clearly indicating that both take almost same time to reach the target. Thus, in this case, the behavior of the resetting trajectory is clearly oscillatory like the original process. In other words, resetting will have almost no effect on the underlying process. Parameter values: set here are  $a = -0.01, \Omega = 1$ .

intrinsic time periods and we observe a significant increase in  $\langle TT_R \rangle$ . To further illustrate this behavior, we now choose two particular values of  $\langle R \rangle$  from the table such that one lowers the transient time while the second one does not provide any significant improvement. At first, we take  $\langle R \rangle = 4.5$  which reduces the transient time (In Fig. 5b, blue line indicates time signal under sharp resetting which is placed in contrast to the original time series in the absence of resetting). Here, we clearly see a very quick convergence to the steady state for the trajectory subject to resetting. On the other hand, when  $\langle R \rangle = 6.5$ , Fig. 5c clearly indicates that the blue line (which is the trajectory under resetting) is quite close to the original time signal (denoted by red solid line). A short segment of the signal is zoomed in below Fig. 5c to further demonstrate the proximity between the trajectories. Thus, in effect, the resultant transient time becomes of the same order as that of the uninterrupted process. In summary, sharp restarts are periodic temporal process which occur always after a fixed time  $\langle R \rangle$ . When this period becomes half or full integer of the intrinsic time period of the system, a sudden rise in mean transient time is observed with the emergence of those consecutive oscillations as seen in Fig. 3 (left panel for  $M_1$ ) in the main text.

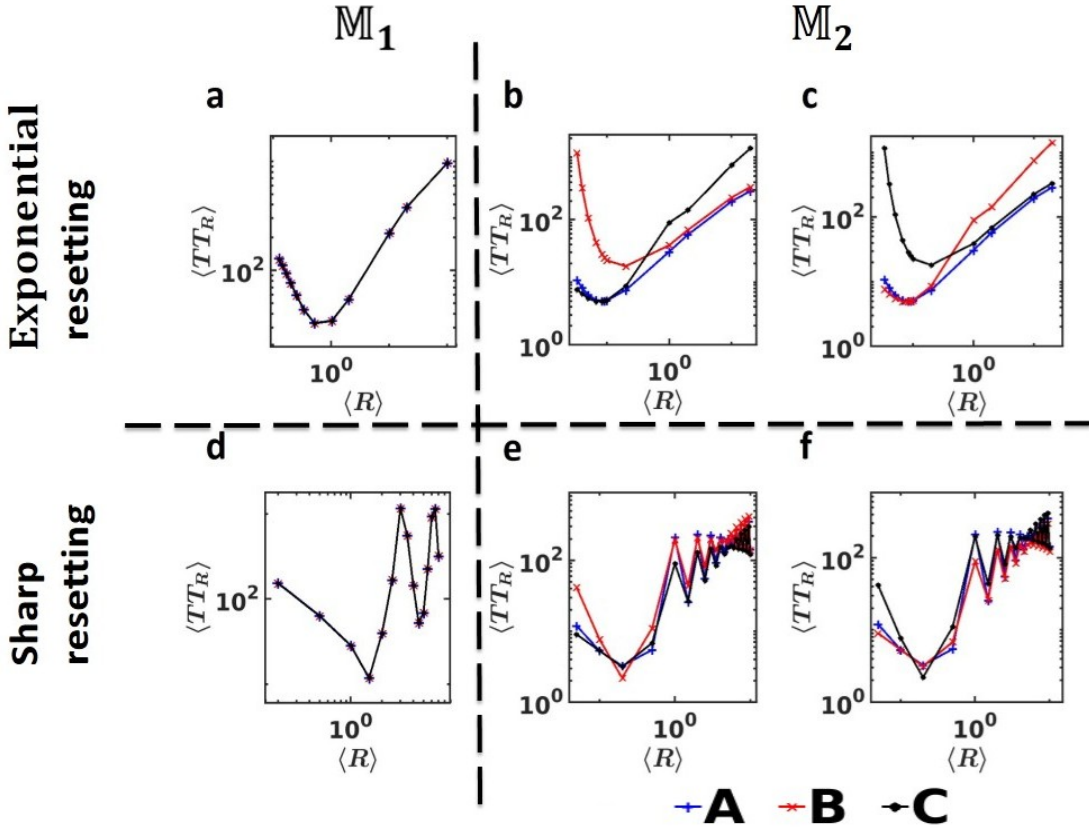


FIG. 6. Variation in mean transient time for different control lines. We have chosen different type of control lines as mentioned in details in Sec. V. For  $\mathbb{M}_1$ , we have considered three different control lines which pass through the points  $A : (4, 0)$ ,  $B : (-2, 4)$ ,  $C : (-4, -2)$  and the equilibrium point  $P : (0, 0)$  respectively. For each of these cases, we have plotted the mean transient time as a function of  $\langle R \rangle$  [panel (a) for exponential and panel (d) for sharp]. We find that there is no effect of different control lines on the mean transient time in  $\mathbb{M}_1$ . In  $\mathbb{M}_2$ , there are two equilibrium points  $P_1 : (7.65942, 7.65942, 22)$  and  $P_2 : (-7.65942, -7.65942, 22)$ . We have also taken three points  $A : (0, 0, 0)$ ,  $B : (20, 20, 30)$ , and  $C : (-20, -20, 30)$  through which control lines pass. Thus, there are two sets of control lines each of which comprises three lines passing through  $A, B, C$  and either  $P_1$  or  $P_2$ . In panel (b) and panel (e), we have plotted  $\langle TT_R \rangle$  as a function of  $\langle R \rangle$  for exponential and sharp resetting respectively using the control lines that pass through  $A, B, C$  and  $P_1$ . We have prepared similar plots in panel (c) and panel (f) where the control lines pass through  $A, B, C$  and  $P_2$ . Here, we see that mean transient time depends on the choice of control lines. This is due to the nature of the basin for the Lorenz system as discussed in details in Sec. VB. Parameter values set here are:  $a = -0.01, \Omega = 1$  (for  $\mathbb{M}_1$ ) and  $\sigma = 10, \rho = 23, \beta = \frac{8}{3}$  (for  $\mathbb{M}_2$ ).

## V. BEHAVIOR OF THE MEAN AND FLUCTUATIONS IN TRANSIENT TIME ON THE CHOICE OF CONTROL LINES

In this section, we investigate in details the ramifications in  $\langle TT_R \rangle$  and fluctuations  $\sigma_R$  on the choice of control lines. Let us first recall that a control line is randomly chosen from the basin of attraction but it always passes through the equilibrium point(s). Here, the analysis is done both for the exponential and sharp resetting. In the following, we discuss the effects of control line on the mean and fluctuations first on the Stuart-Landau system ( $\mathbb{M}_1$ ), and then on the Lorenz system ( $\mathbb{M}_2$ ).

### A. Effect of control lines on $\mathbb{M}_1$

In system  $\mathbb{M}_1$ , the equilibrium point is located at  $(0, 0)$  which we denote as  $P$ . In the main text, we choose the control line randomly from the basin such that it passes through  $(4, 4)$  and the equilibrium point  $P$ . We have shown that this protocol yields a significant reduction in mean and fluctuations in transient time. To show that this behavior is invariant to the choice of the control line, we now construct the following control lines which pass through

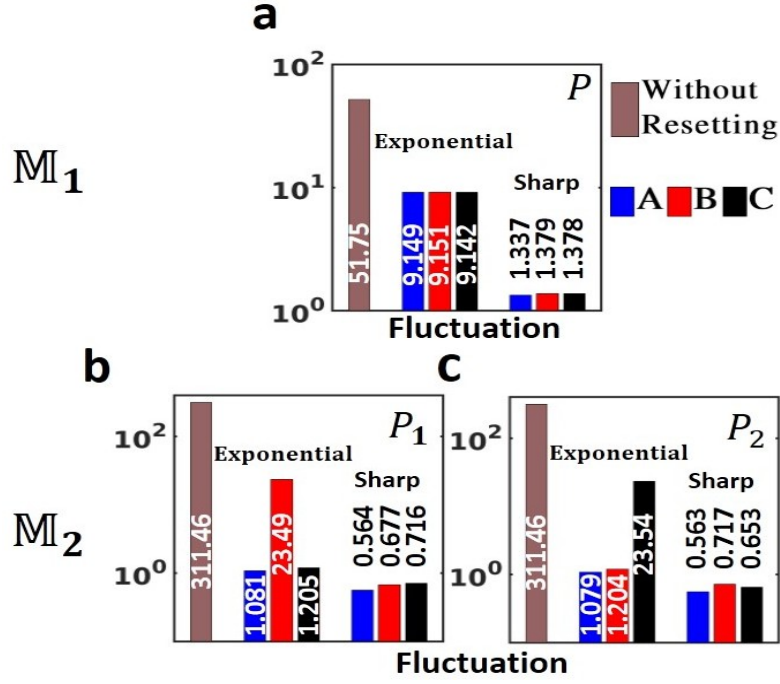


FIG. 7. Variation in fluctuations for different choices of control lines. In panel (a), we have shown a bar plot comparison of fluctuations between the original dynamics and resetting induced dynamics in  $M_1$ . Resetting was conducted at  $\langle R \rangle = 1$  (both for exponential and sharp resetting) by taking the control lines which pass through  $P$  and  $A, B, C$  respectively (see Sec. VA). It is clear from the figure that (i) resetting reduces fluctuations and (ii) the magnitude of the fluctuations is almost same implying that resetting does not depend on the choice of control lines in  $M_1$ . This observation is in accordance with Fig. 6a and Fig. 6d. Panel (b) and panel (c) show bar plot comparison of fluctuations between the original dynamics and resetting induced dynamics in  $M_2$  (conducted at  $\langle R \rangle = 0.1$ ) when the control lines pass through  $A, B, C$  and either  $P_1$  or  $P_2$  respectively (see Sec. VB). We concur with the observation that resetting also reduces fluctuations in this case. However, the magnitudes of fluctuations are different in each case, as expected, due to the underlying non-uniform structure of the basin in Lorenz system. Parameter values set here are:  $a = -0.01, \Omega = 1$  (for  $M_1$ ) and  $\sigma = 10, \rho = 23, \beta = \frac{8}{3}$  (for  $M_2$ ).

the random coordinates mentioned below from the basin of attraction:

1.  $P(0,0)$  and  $A(4,0)$ ,
2.  $P(0,0)$  and  $B(-2,4)$ ,
3.  $P(0,0)$  and  $C(-4,-2)$ .

For each of the cases above, we have plotted  $\langle TT_R \rangle$  as a function of  $\langle R \rangle$  for the exponential (Fig. 6a) and sharp resetting (Fig. 6d) respectively. First, we note that indeed resetting reduces the mean transient time. Secondly, it becomes evident from the plots that all the curves collapse thus clearly indicating the fact that the variation in mean transient time does not depend on the choice of the control line, particularly, for case of  $M_1$ , where the basin of attraction is homogeneous, and thus the system can not distinguish between the choice of the control lines. In Fig. 7a, we have shown a comparison between the fluctuations in the original dynamics and with resetting dynamics (both for exponential and sharp) for given  $\langle R \rangle = 1$ . Note that the fluctuations are now reduced due to the resetting. Moreover, since the basin is uniform, the choice of control line did not have any impact on the fluctuations similar to the mean as seen above.

### B. Effect of control lines on $M_2$

To see the effects of control lines on  $M_2$ , we first recall that  $M_2$  has two fixed points ( $P_1$  and  $P_2$ ) which are stable for a certain range of  $\rho$  (See the Sec. II B). The system  $M_2$  has riddle basin of attraction for the equilibrium points  $P_1$  and  $P_2$ . As was mentioned in the main text, in this case, we have some flexibility in choosing control lines e.g., it can pass through one of the equilibrium points ( $P_1$  or  $P_2$ ) or via both. We discuss each of the cases in the following.

1. *Effect of fixed control line passing through both  $P_1$  and  $P_2$*

We first discuss the case when the control line passes through both the equilibrium points  $P_1$  and  $P_2$ . We compute the transient time when the trajectory reaches any of these points. This scenario was already discussed in the main text. In particular, we choose the control line such that it passes through  $P_1(7.65942, 7.65942, 22)$  and  $P_2(-7.65942, -7.65942, 22)$ . When conducted at  $\langle R \rangle = 0.1$ , a net reduction in mean and fluctuations was observed.

2. *Effect of fixed control line passing through  $P_1$*

In this case, we choose control lines that pass through the equilibrium point  $P_1$ , which is the only target. Here, we take three random control lines passing through the following points from the basin of attraction as described below

1.  $P_1(7.65942, 7.65942, 22)$  and  $A(0, 0, 0)$ ,
2.  $P_1(7.65942, 7.65942, 22)$  and  $B(20, 20, 30)$ ,
3.  $P_1(7.65942, 7.65942, 22)$  and  $C(-20, -20, 30)$ .

In Figs. 6b and 6e, we have plotted  $\langle TT_R \rangle$  as a function of  $\langle R \rangle$  for the exponential and deterministic resetting respectively. The behavior is similar to Fig. 3 in the main text which essentially reiterates the fact that resetting reduces the mean transient time. In Fig. 7b, we have shown a comparison between the fluctuations in the original dynamics and with resetting dynamics (both for exponential and sharp) for given  $\langle R \rangle = 0.1$  and choice of the control lines as mentioned above. In here, we also see that resetting lowers the fluctuations.

3. *Effect of fixed control line passing through  $P_2$*

In this case we take the control line passing through the equilibrium point  $P_2$  (which is the only target) and the following other points

1.  $P_2(-7.65942, -7.65942, 22)$  and  $A(0, 0, 0)$ ,
2.  $P_2(-7.65942, -7.65942, 22)$  and  $B(20, 20, 30)$ ,
3.  $P_2(-7.65942, -7.65942, 22)$  and  $C(-20, -20, 30)$ .

Here too, we find that resetting using a control line technique reduces the mean transient time. These conclusions are in accordance with the Figs. 6c and 6f which show the variation of mean transient time as a function of  $\langle R \rangle$ . In Fig. 7c, we have shown a comparison between the fluctuations in the original dynamics and with resetting dynamics (both for exponential and sharp) for given  $\langle R \rangle = 0.1$  and choice of the control lines as mentioned above. In here, we also see that resetting lessens the fluctuations.

As a final remark, we note that since the basin of  $\mathbb{M}_2$  is non-homogeneous, we do not observe any collapse for the mean transient time for different choices of control lines as was seen in the case of  $\mathbb{M}_1$ .

## VI. IMPACT OF CONTROL PARAMETERS ON THE TRANSIENT TIME NEAR THE CRITICAL TRANSITION

It is well known that in non-linear systems, the parameters play a paramount role to decide the structure of the basin, attractor or fixed points. For our current models, we have already discussed in Sec. II that the controlling parameters can change the structure of the attractor qualitatively i.e., transform the stable fixed points into limit cycle or chaos (beyond critical values). But it is important to note that as the parameters are tuned to the critical values, duration of transient states gradually increases. For example, it is known that the average lifetime or transient time of a chaotic transient depends critically upon the system parameter i.e., it diverges as a power law form near the critical point [1]. Naturally, the question appears on how the situation changes in the presence of resetting near the critical point and what are the overall ramifications of the resetting strategies (exponential and sharp) on the statistics of the transient time. In this section, we have examined these issues in details.

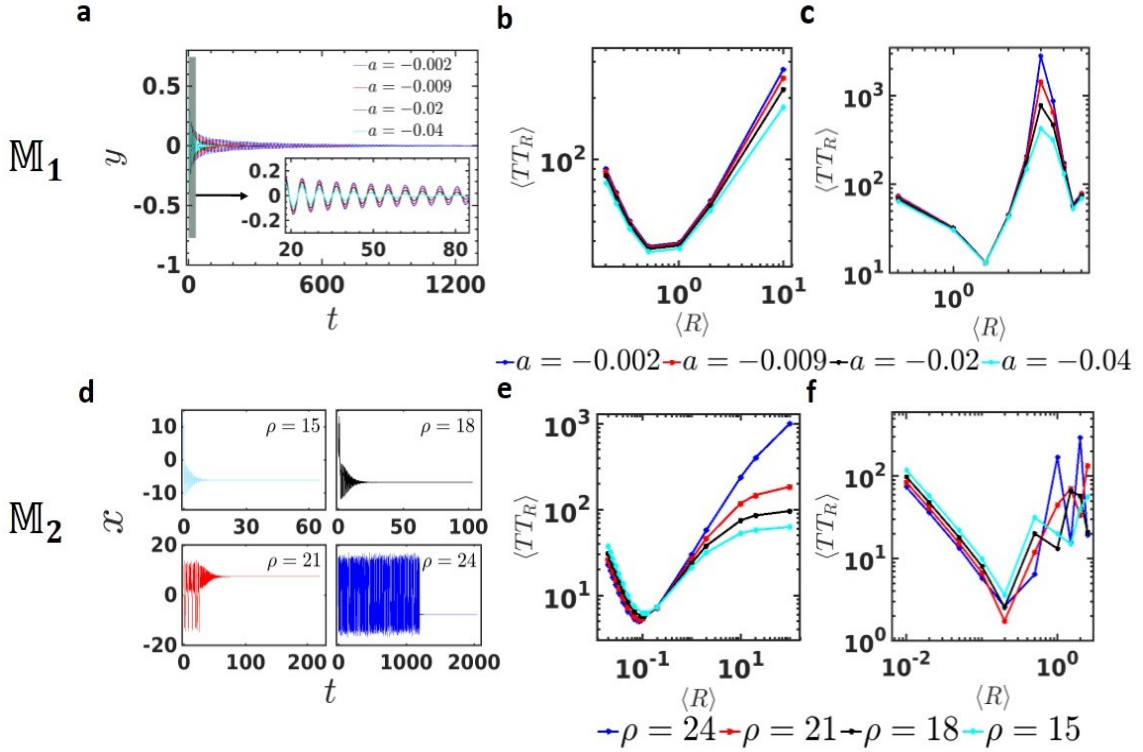


FIG. 8. Mean transient time regulation by resetting near the critical transition. Panel (a) and panel (d) show four time series of the original dynamics for  $M_1$  and  $M_2$  respectively. In panel (a), the trajectories in coordinate  $y$  are plotted as a function of time for different values of  $a$  (shown in the plot) near the critical transition  $a_c = 0$ . In panel (d), the trajectories in coordinate  $x$  are plotted as a function of time for different values of  $\rho$  (shown in the plot) near the critical transition  $\rho_c = 24.06$ . The varying parameters are  $a = -0.002$  (blue),  $-0.009$  (red),  $-0.02$  (black),  $-0.04$  (cyan), and  $\rho = 15$  (cyan),  $18$  (black),  $21$  (red),  $24$  (blue). In panel (b) and (c), we have plotted  $\langle TT_R \rangle$  as a function of  $\langle R \rangle$  for exponential and sharp resetting for the above mentioned values of  $a$ . Similarly, panel (e) and panel (f) depict variation of  $\langle TT_R \rangle$  as a function of  $\langle R \rangle$  for exponential and sharp resetting for the above mentioned values of  $\rho$ . Other parameters set for the simulations are:  $\Omega = 1$  (for  $M_1$ ), and  $\sigma = 10$ ,  $\beta = \frac{8}{3}$  (for  $M_2$ ).

### A. System $M_1$

In the Stuart-Landau oscillatory system, we regulate the decay parameter  $a$  which determines whether the system has a limit cycle or a fixed point. Following analysis from Sec. II A, we know that this transition occurs exactly at  $a_c = 0$ . In what follows, we scan  $a$  for a range of values close to  $a_c$  and examine the variations due to resetting. For a given initial condition, the transient time of the underlying process gradually increases as we increase  $a$ . This is shown in Fig. 8a where  $a$  has assumed four different values  $-0.002, -0.009, -0.02, -0.04$  and clearly, as  $|a|$  increases the decay rate of the oscillation increases and we see a faster convergence (i.e., a shorter transient time) to the steady state (see inset in Fig. 8a). To add restart, we follow the same protocol (by resetting at the control line that passes through the equilibrium point  $P$ ) as outlined in the main text to this dynamics but when  $a$  is close to  $a_c$ . In Fig. 8b, we have plotted  $\langle TT_R \rangle$  as a function of  $\langle R \rangle$  [ $a = -0.002$  (blue),  $-0.009$  (red),  $-0.02$  (black), and  $-0.04$  (cyan)] when the resetting is exponential. The plot clearly shows that  $\langle TT_R \rangle$  is significantly reduced near the critical transition. Moreover, in each case above, we find an optimal resetting time  $\langle R^* \rangle$  which makes  $\langle TT_R \rangle$  to be minimum (see Table I for exponential and Table II for sharp resetting and details of the mean transient time at the optimality). We prepare a plot in Fig. 8c for the sharp resetting case where we find behavior of  $\langle TT_R \rangle$  to be similar. The oscillatory behavior, as was discussed in Sec. IV, was noted for the sharp resetting.

## B. System $\mathbb{M}_2$

In the Lorenz system, it is known that the Rayleigh number  $\rho$  marks the critical transition between the chaotic transient phase and chaotic attractor [1, 3]. For fixed parameters  $\sigma = 10$  and  $\rho = \frac{8}{3}$ , the system exhibits transient chaos in the range of  $\rho \in (1.926, 24.06)$  where the transition to a chaotic attractor takes place at  $\rho_c = 24.06$ . To demonstrate the effects of resetting near the critical transition, we take four different values for  $\rho$  and plot the trajectories for each of them. We demonstrate in Fig. 8d, trajectories in  $x$ -coordinates as a function of time for  $\rho = 24$  (blue), 21 (red), 18 (black), and 15 (cyan). Here, chaotic transient phase persists longer as we increase  $\rho$  close to  $\rho_c$ . To illustrate the effects of resetting, we plot  $\langle TT_R \rangle$  as a function of  $\langle R \rangle$  for each of the cases above (by taking a control line which passes through both the equilibrium points  $P_1$  and  $P_2$ ). Both for exponential (Fig. 8e) and sharp resetting (Fig. 8f), we observe that resetting reduces the transient time which would be significantly higher and even diverging (close to  $\rho_c$ ). Moreover, emergence of an optimal resetting rate  $\langle R^* \rangle$  was observed in each case (see Table I for exponential and Table II for sharp resetting and details of the mean transient time at the optimality).

	$a$	$\langle TT_R^* \rangle$	$\rho$	$\langle TT_R^* \rangle$
Table I	-0.04	35.40	15	6.16
	-0.02	36.63	18	5.70
	-0.009	37.34	21	5.30
	-0.002	37.81	24	5.05

	$a$	$\langle TT_R^* \rangle$	$\rho$	$\langle TT_R^* \rangle$
Table II	-0.04	12.905	15	3.59
	-0.02	13.02	18	2.55
	-0.009	13.07	21	1.74
	-0.002	13.10	24	2.59

Finally, we conclude this section by reemphasizing the fact that resetting has a strong impact on the average transient times even close to the critical transition. In particular, resetting renders the mean transient time lower near the critical point which are otherwise large or diverging. It is worth emphasizing that resetting also regulates the fluctuations strongly near the critical transition. We refer to the barplot in Fig. 9 which clearly shows that there is a significant reduction in fluctuations even when we modulate the parameters very close to the critical transition. A consistent limit is obtained for  $\langle R \rangle \geq 10$ , where the system behaves as it would in the absence of resetting.

## VII. COMPUTATIONAL METHOD

In this section, we briefly discuss the computational method that has been used to gather statistics and perform averaging on the transient time under exponential (stochastic) and sharp (deterministic) resetting strategy.

- **Step I. Fix the target:** First, we determine the equilibrium point  $\mathcal{A}$  of the given differential equation. There can be many equilibrium points in the system, but we may choose one or many of them to be the target points. For brevity, let us denote the specific targeted fixed point by  $\mathbf{x}_f$ .
- **Step II. Integration scheme:** To integrate the deterministic model, we choose a random initial condition, say  $\mathbf{x}_0$  from the basin of attraction  $\mathcal{B}_{\mathcal{A}}$  at the initial time  $T_0$ . The 4-th order Runge-Kutta method is used to simulate the system with fixed step length  $h = 0.01$ . Sufficient number of data points are generated such that trajectory reaches to its target with a close vicinity measured by  $\epsilon = 10^{-9}$  i.e., it satisfies Eq. 4 in the main text.
- **Step III. Generating resetting times:** Starting from  $T_0$ , we now evolve the dynamics under resetting mechanism. Resetting events occur at time  $T_1, T_2, T_3, \dots$ , where the duration between two consecutive events (

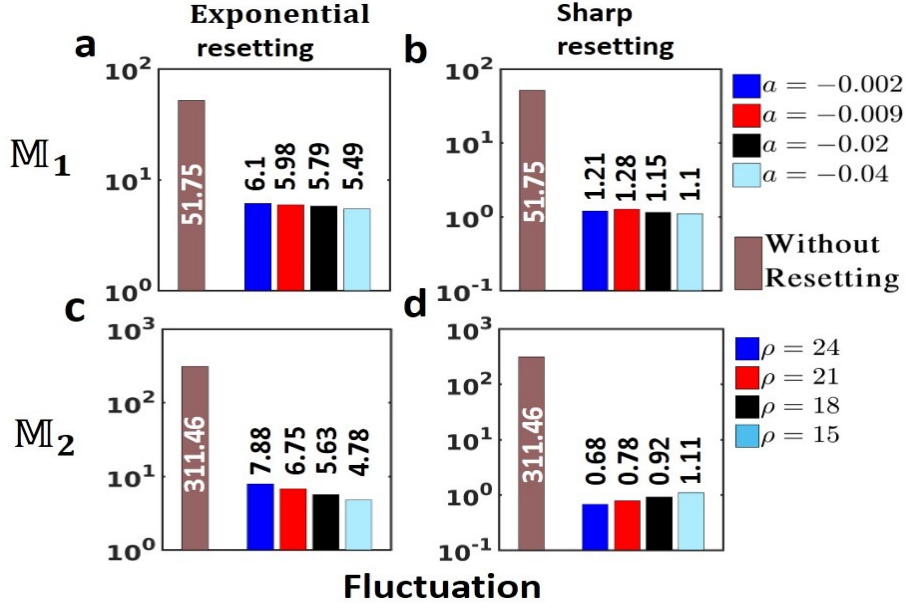


FIG. 9. Fluctuation regulation by resetting near the critical transition. In this figure, we present bar plot comparison between the fluctuations of the original and reset induced dynamics. For  $M_1$ , while conducted at  $\langle R \rangle = 1$ , we observe that both exponential (panel a) and sharp (panel b) resetting strategies have reduced the fluctuations even when we are close to the critical transition  $a = a_c = 0$ . Similar bar plot is laid out for  $M_2$  but resetting here was conducted at  $\langle R \rangle = 0.1$ . Here too, we find that resetting remains beneficial to reduce fluctuations as we scan  $\rho$  to its critical value  $\rho_c = 24.06$ .

$\Delta_T : \{T_1 - T_0, T_2 - T_1, T_3 - T_2, \dots\}$  are extracted from an exponential distribution

$$f_R(\Delta_T) = \langle R \rangle^{-1} e^{-\frac{\Delta_T}{\langle R \rangle}}, \quad \text{where } \langle R \rangle \text{ is the mean} \quad (13)$$

and periodic distribution for sharp resetting

$$f_R(\Delta_T) = \delta(\Delta_T - \langle R \rangle), \quad \text{where } \langle R \rangle \text{ is the fixed time period.} \quad (14)$$

For numerical schemes, the resetting times were generated at the discrete points:  $\frac{1}{h} \times \{T_1, T_2, T_3, \dots\}$ .

- **Step IV. Fixing a control line:** An arbitrary point  $\mathbf{x}_c$  is randomly chosen from the basin of attraction and we draw a straight line passing through  $\mathbf{x}_c$  and any of the equilibrium point(s), say,  $\mathbf{x}_f$ . This arbitrary control line is kept fixed for the entire scanning process. We have scanned the transient times of  $5 \times 10^6$  initial states for each  $\langle R \rangle$ .
- **Step V. Projection procedure:** To describe the projection or resetting to the control line, let us first assume that resetting occurred at some time  $T_i$ , and at this very moment, coordinate of the trajectory is  $\mathbf{x}_1$ . To decide, where to reset in the control line, we choose a point  $\mathbf{x}_2$  from the control line such that the line passing through  $\mathbf{x}_1$  and  $\mathbf{x}_2$  will be perpendicular to the control line. If this condition is satisfied, we project the coordinate  $\mathbf{x}_1$  to  $\mathbf{x}_2$ . This process is repeated for other resetting events.
- **Step VI. Calculation of transient time:** We stop our simulation after reaching at  $\mathbf{x}_n$  after  $n$ -th iteration only if the condition  $\|\mathbf{x}_f - \mathbf{x}_n\| < \epsilon$  ( $= 10^{-9}$ ) (See Sec. I and Eq. (2) in the main text) is satisfied. Subsequently, the transient time will be  $TT = n \times h$ . This time is random, and we generate histogram of the transient time from many such realizations.

Following the steps I-VI, we collect data of the required observables and investigate various statistical properties.

## VIII. SUMMARY OF THE NUMERICAL VALUES USED IN THE MAIN TEXT

In this section, we provide numerical values for the mean and fluctuations for exponential and sharp resetting as was discussed in the main text. We refer to Fig. 10 which contains a table listing the exact values.



	Without resetting		Exponential resetting		Sharp resetting		
	$\langle TT \rangle$	$\sigma$	$\langle R \rangle$	$\langle TT_R \rangle$	$\sigma_R$	$\langle TT_R \rangle$	$\sigma_R$
$\mathbb{M}_1$	1786.9	51.75	1	38.67	9.15	32.08	0.34
$\mathbb{M}_2$	640.57	311.46	0.1	5.12	1.08	6.06	0.71

FIG. 10. Numerical values for the mean and fluctuations as was pointed out in the main text. In  $\mathbb{M}_1$ , both resetting strategies (exponential and sharp) were conducted at  $\langle R \rangle = 1$  (also see Fig. 2e in the main text for the exponential resetting). In  $\mathbb{M}_2$ , everything was similar but we took  $\langle R \rangle = 0.1$  (also see Fig. 2j in the main text for the exponential resetting). In both the cases (exponential and sharp), the order of improvement in mean and fluctuations was mentioned in the main text.

- 
- [1] C. Grebogi, E. Ott, and J. A. Yorke, *Physical Review Letters* **57**, 1284 (1986).  
[2] Y.-C. Lai and T. Tél, *Transient chaos: complex dynamics on finite time scales*, Vol. 173 (Springer Science & Business Media, 2011).  
[3] J. A. Yorke and E. D. Yorke, *Journal of Statistical Physics* **21**, 263 (1979).  
[4] E. G. Altmann, J. S. Portela, and T. Tél, *Reviews of Modern Physics* **85**, 869 (2013).  
[5] T. Lilienkamp, J. Christoph, and U. Parlitz, *Physical Review Letters* **119**, 054101 (2017).  
[6] T. Lilienkamp and U. Parlitz, *Physical Review Letters* **120**, 094101 (2018).  
[7] T. M. Lenton, *Nature Climate Change* **1**, 201 (2011).  
[8] M. Scheffer, J. Bascompte, W. A. Brock, V. Brovkin, S. R. Carpenter, V. Dakos, H. Held, E. H. Van Nes, M. Rietkerk, and G. Sugihara, *Nature* **461**, 53 (2009).  
[9] A. Hastings, K. C. Abbott, K. Cuddington, T. Francis, G. Gellner, Y.-C. Lai, A. Morozov, S. Petrovskii, K. Scranton, and M. L. Zeeman, *Science* **361**, eaat6412 (2018).  
[10] A. Morozov, K. Abbott, K. Cuddington, T. Francis, G. Gellner, A. Hastings, Y.-C. Lai, S. Petrovskii, K. Scranton, and M. L. Zeeman, *Physics of Life Reviews* **32**, 1 (2019).  
[11] A. Gosztolai, J. A. Carrillo, and M. Barahona, *Frontiers in Physics* **6**, 153 (2019).  
[12] R. Martin, M. Schlüter, and T. Blenckner, *Proceedings of the National Academy of Sciences* **117**, 2717 (2020).  
[13] C. Hens, U. Harush, S. Haber, R. Cohen, and B. Barzel, *Nature Physics* **15**, 403 (2019).  
[14] W. Tarnowski, I. Neri, and P. Vivo, *Physical Review Research* **2**, 023333 (2020).  
[15] A. Hastings, *Trends in Ecology & Evolution* **19**, 39 (2004).  
[16] A. Hastings, *Ecology* **91**, 3471 (2010).  
[17] S. N. Majumdar, A. Pal, and G. Schehr, *Physics Reports* **840**, 1 (2020).  
[18] A. Vanselow, S. Wicczorek, and U. Feudel, *Journal of Theoretical Biology* **479**, 64 (2019).  
[19] M. Scheffer, S. Carpenter, J. A. Foley, C. Folke, and B. Walker, *Nature* **413**, 591 (2001).  
[20] J.-F. Arnoldi, A. Bideault, M. Loreau, and B. Haegeman, *Journal of Theoretical Biology* **436**, 79 (2018).  
[21] J. Gao, B. Barzel, and A.-L. Barabási, *Nature* **530**, 307 (2016).  
[22] A. E. Motter, S. A. Myers, M. Anghel, and T. Nishikawa, *Nature Physics* **9**, 191 (2013).  
[23] S. Redner, *A guide to first-passage processes* (Cambridge University Press, 2001).  
[24] A. J. Bray, S. N. Majumdar, and G. Schehr, *Advances in Physics* **62**, 225 (2013).  
[25] R. Metzler, G. Oshanin, and S. Redner, *First-Passage Phenomena and Their Applications* (World Scientific, 2014).  
[26] O. Bénichou, C. Loverdo, M. Moreau, and R. Voituriez, *Reviews of Modern Physics* **83**, 81 (2011).  
[27] F. Mori, P. Le Doussal, S. N. Majumdar, and G. Schehr, *Physical Review Letters* **124**, 090603 (2020).  
[28] O. Bénichou, C. Chevalier, J. Klafter, B. Meyer, and R. Voituriez, *Nature Chemistry* **2**, 472 (2010).  
[29] S. Condamin, O. Bénichou, V. Tejedor, R. Voituriez, and J. Klafter, *Nature* **450**, 77 (2007).  
[30] N. Levernier, M. Dolgushev, O. Bénichou, R. Voituriez, and T. Guérin, *Nature Communications* **10**, 1 (2019).  
[31] T. Guérin, N. Levernier, O. Bénichou, and R. Voituriez, *Nature* **534**, 356 (2016).  
[32] M. R. Evans, S. N. Majumdar, and G. Schehr, *Journal of Physics A: Mathematical and Theoretical* **53**, 193001 (2020).  
[33] M. R. Evans and S. N. Majumdar, *Physical Review Letters* **106**, 160601 (2011).  
[34] M. R. Evans and S. N. Majumdar, *Journal of Physics A: Mathematical and Theoretical* **44**, 435001 (2011).  
[35] S. Reuveni, *Physical Review Letters* **116**, 170601 (2016).  
[36] A. Pal and S. Reuveni, *Physical Review Letters* **118**, 030603 (2017).  
[37] A. Pal, I. Eliazar, and S. Reuveni, *Physical Review Letters* **122**, 020602 (2019).  
[38] S. Belan, *Physical Review Letters* **120**, 080601 (2018).  
[39] A. Pal, A. Kundu, and M. R. Evans, *Journal of Physics A: Mathematical and Theoretical* **49**, 225001 (2016).

- [40] S. Reuveni, M. Urbakh, and J. Klafter, *Proceedings of the National Academy of Sciences* **111**, 4391 (2014).
- [41] M. Luby, A. Sinclair, and D. Zuckerman, *Information Processing Letters* **47**, 173 (1993).
- [42] A. Montanari and R. Zecchina, *Physical Review Letters* **88**, 178701 (2002).
- [43] L. Kusmierz, S. N. Majumdar, S. Sabhapandit, and G. Schehr, *Physical Review Letters* **113**, 220602 (2014).
- [44] A. Falcón-Cortés, D. Boyer, L. Giuggioli, and S. N. Majumdar, *Physical Review Letters* **119**, 140603 (2017).
- [45] A. Chechkin and I. Sokolov, *Physical Review Letters* **121**, 050601 (2018).
- [46] G. J. Lapeyre and M. Dentz, *Physical Chemistry Chemical Physics* **19**, 18863 (2017).
- [47] A. Pal and V. V. Prasad, *Physical Review E* **99**, 032123 (2019).
- [48] D. Boyer and C. Solis-Salas, *Physical Review Letters* **112**, 240601 (2014).
- [49] U. Bhat, C. De Bacco, and S. Redner, *Journal of Statistical Mechanics: Theory and Experiment* **2016**, 083401 (2016).
- [50] E. G. Ritchie and C. N. Johnson, *Ecology Letters* **12**, 992 (2009).
- [51] S. Dharmaraja, A. Di Crescenzo, V. Giorno, and A. G. Nobile, *Journal of Statistical Physics* **161**, 326 (2015).
- [52] V. Lucarini, D. Faranda, J. M. M. de Freitas, M. Holland, T. Kuna, M. Nicol, M. Todd, S. Vaienti, *et al.*, *Extremes and recurrence in dynamical systems* (John Wiley & Sons, 2016).
- [53] N. L. Lundström, *Nonlinear Dynamics* **93**, 887 (2018).
- [54] V. V. Klinshov, S. Kirillov, J. Kurths, and V. I. Nekorkin, *New Journal of Physics* **20**, 043040 (2018).
- [55] T. Kittel, J. Heitzig, K. Webster, and J. Kurths, *New Journal of Physics* **19**, 083005 (2017).
- [56] **See Supplemental Material for detailed description of the models, derivations, additional figures and computational method.**
- [57] S. Gupta, S. N. Majumdar, and G. Schehr, *Physical Review Letters* **112**, 220601 (2014).
- [58] A. Pal, *Physical Review E* **91**, 012113 (2015).
- [59] V. Méndez and D. Campos, *Physical Review E* **93**, 022106 (2016).
- [60] A. Pal and V. V. Prasad, *Physical Review Research* **1**, 032001 (2019).
- [61] S. Eule and J. J. Metzger, *New Journal of Physics* **18**, 033006 (2016).
- [62] D. Gupta, C. A. Plata, and A. Pal, *Physical Review Letters* **124**, 110608 (2020).
- [63] Y. Kuramoto, *Chemical oscillations, waves, and turbulence* (Courier Corporation, 2003).
- [64] A. Pikovsky, J. Kurths, M. Rosenblum, and J. Kurths, *Synchronization: a universal concept in nonlinear sciences*, Vol. 12 (Cambridge university press, 2003).
- [65] E. N. Lorenz, *Journal of the Atmospheric Sciences* **20**, 130 (1963).
- [66] E. Ott, *Chaos in dynamical systems* (Cambridge university press, 2002).
- [67] S. Strogatz, *Nonlinear dynamics and chaos* (Avalon Publishing, 2016).
- [68] A. Pal, L. Kuśmierz, and S. Reuveni, *New Journal of Physics* **21**, 113024 (2019).